International Journal of Nanomedicine

Dovepress
open access to scientific and medical research

Open Access Full Text Article

ORIGINAL RESEARCH

Oral Exposure to ZnO Nanoparticles Disrupt the Structure of Bone in Young Rats via the OPG/RANK/RANKL/IGF-1 Pathway

This article was published in the following Dove Press journal:
International Journal of Nanomedicine

Xinyue Xu[1,*]
Yizhou Tang[2,*]
Yuanyuan Lang[3,*]
Yanling Liu[1]
Wenshu Cheng[1]
Hengyi Xu[2]
Yang Liu[1]

[1]Department of Pediatrics, The Second Affiliated Hospital of Nanchang University, Nanchang 330006, People's Republic of China; [2]State Key Laboratory of Food Science and Technology, Nanchang University, Nanchang 330047, People's Republic of China; [3]Medical Imaging Center, The Second Affiliated Hospital of Nanchang University, Nanchang 330006, Jiangxi Province, People's Republic of China

*These authors contributed equally to this work

Purpose: To evaluate the effects of ZnO NPs on bone growth in rats and explore the possible mechanisms of action.

Materials and Methods: Three-week-old male rats received ultrapure water or 68, 203, and 610 mg/kg zinc oxide nanoparticles (ZnO NPs) for 28 days, orally.

Results: The high-dosage groups caused significant differences in weight growth rate, body length, and tibia length ($P<0.05$), all decreasing with increased ZnO NP dosage. There were no significant differences in body mass index (BMI) ($P>0.05$). The zinc concentration in liver and bone tissue increased significantly with increased ZnO NP dosage ($P<0.05$). Clearly increased aspartate aminotransferase (AST) and alanine aminotransferase (ALT) levels were observed in the 610 mg/kg ZnO NP group ($P>0.05$), whereas alkaline phosphatase (ALP) increased in the 610 mg/kg ZnO NP group ($P<0.05$). Significant differences in insulin-like growth factor type 1 (IGF-1) levels and a decrease in calcium (Ca) levels were observed in 203 and 610 mg/kg ZnO NP groups ($P<0.05$). Phosphorus (P) levels increased and the Ca/P ratio decreased in the 610 mg/kg ZnO NP group ($P<0.05$). Micro-computed tomography (micro-CT) of the tibia demonstrated signs of osteoporosis, such as decreased bone density, little trabecular bone structure and reduced cortical bone thickness. Micro-CT data further demonstrated significantly decreased bone mineral density (BMD), trabecular number (Tb.N), and relative bone volume (BV/TV) with increasing dosage of ZnO NPs. Osteoprotegerin (OPG) expression and the ratio of OPG to receptor activator of nuclear factor-κB ligand (RANKL) were statistically lower in the 610 mg/kg ZnO NP group ($P<0.05$), whereas RANKL expression did not change significantly ($P>0.05$).

Conclusion: We infer that ZnO NPs affect bone growth in young rats directly or indirectly by altering IGF-1 levels. Overall, the results indicate that ZnO NPs promote osteoclast activity and increase bone loss through the OPG/RANK/RANKL/IGF-1 pathway.

Keywords: ZnO NPs, young rats, bone growth, OPG/RANK/RANKL/IGF-1 pathway

Correspondence: Yang Liu
Department of Pediatrics, The Second Affiliated Hospital of Nanchang University, No. 1 Minde Road, Donghu District, Nanchang 330006 Jiangxi Province, People's Republic of China
Tel +86-791-8631-1209
Email ocean3166@yeah.net

Hengyi Xu
State Key Laboratory of Food Science and Technology, Nanchang University, 235 Nanjing East Road, Nanchang 330047, People's Republic of China
Tel +86-791-8830-4447-ext-9520
Fax +86-791-8830-4400
Email kidyxu@163.com

Introduction

Nanoparticles (NPs) are defined as particles falling within the nanometer-scale, ranging from 1 to 100 nm in diameter.[1] They are used extensively in a variety of fields of biology and medicine, in addition to within the manufacture of food, cosmetics, and everyday consumables.[2] More than 800 consumer products that contain NPs are listed on the Woodrow Wilson Center database.[3] Of these NPs, those based on zinc oxide nanoparticles (ZnO NPs) are reportedly the most widely used nanomaterials.[4] ZnO NPs are used in food additives[5] and can thus enter the

human body through the food chain.[6] ZnO NPs are also used in everyday consumables, such as in cosmetics, medicines, ceramics, and pigments,[7] in addition to children's products such as pacifiers, teddy bears, and other basic products.[8] Using products that contain ZnO NPs increases the risk of exposure.[9]

Given the wide-ranging applications for nanotechnology and the use of nanoproducts, the potential health risks of ZnO NPs, especially to children, require thorough evaluation. In China, each child whose height is two standard deviations less than the mean height of children of the same sex, age, and race are considered to have a short stature.[10] The age-standardized prevalence of short stature is 3.70% in China.[11] A number of studies have found that short stature may affect the physical and mental health of children, especially boys.[12] Bone development is regulated by growth hormone, thyroid hormone, and estrogen. Growth hormone affects bone growth through insulin-like growth factor type 1 (IGF-1). A previous study used the frailty index of osteoporotic fractures and found that the frail group exhibited a low level of IGF-1.[13] The results in another study indicated that bone length, rate of formation, and bone mineral density (BMD) were increased by IGF-1.[14] Yang et al established that short stature caused by the deficiency of growth-hormone reduced bone density and bone strength.[15] Thus, IGF-1 plays an important role in bone growth of children and it is a developmental factor to which clinicians should pay great attention.

Drugs, chemicals, and other environmental agents reportedly have toxic effects on bone tissue.[16,17] Many previous studies have explored the toxicity of ZnO NPs, such as damage to liver function,[18] intestinal microenvironment, intestinal epithelium,[19] and fetal growth and development.[20] But there were few studies to explore the toxicity between the bone tissue and ZnO NPs. Notably, one study suggested that ZnO NPs can increase bone resorption and decrease bone formation, thereby leading to bone loss.[21] However, the mechanism was not clear. Besides, few studies have focused on the effects of ZnO NPs on bone in young animal models of development, especially to bone longitudinal growth.

Therefore, given the potential risks posed by ZnO NPs to the development of bone, especially in children, their toxicity should be urgently explored. In the present study, the influence of ZnO NPs on bone growth and development by its oral exposure to young (three-week-old) male rats were investigated.

Materials and Methods

Preparation of ZnO NPs

The ZnO NPs used in the present study were purchased from Xiya Reagent, LLC (Chengdu, China). The mean diameter and size distribution of the ZnO NPs were measured using scanning electron microscopy (SEM) with Nano Measurer software, as described in previous studies.[18,22,23] Powdered ZnO NPs (27.5nm±4.1nm) were weighted and added into ultrapure water for dissolving. The mixture was ultrasonicated for half an hour to produce an even dispersion.

Animals

Ten pregnant female Sprague–Dawley rats (SD rats) were purchased from the Experimental Animal Center of Nanchang University (Nanchang, China). All experimental procedures involving animals were approved by the Animal Care Review Committee (approval number 0064257), Nanchang University, Jiangxi, China, which adhered to the institutional animal-care committee guidelines.

Rat offspring were breastfed on the day immediately postnatal (PND 1). Prior to weaning (PND 21), 32 young male rats were randomized into four groups (n = 8), namely, three ZnO NP treatment groups and one control group. They were maintained at room temperature (25°C) in a 12 h light-dark cycle with unlimited water and feed. Each young SD rat was marked on their tail, back, and feet for easy identification.

Experimental Design

Nutritional zinc (Zn) is used as a supplement to prevent and treat human diseases, especially in children.[24] In the food industry, ZnO NPs have replaced ZnO as an additive to enhance bioavailability.[25] Thus, the oral toxicity of ZnO NPs requires additional investigation. In the present study, three-week-old SD rats were studied.[26,27] The highest dosage of Zn allowed in children is 7 mg/d.[28] The dosage in rats, 100-fold greater than the maximum dosage for children was based on an additional safety factor stated by a number of toxicologists.[26] In addition to this, we aimed to find a harmful threshold for ZnO NPs in animals undergoing bone growth. Accordingly, 610 mg/kg was selected as the highest dosage in the present study and decreased it three and nine-fold for two other dosage groups.

The young SD rats in the experimental groups received different doses of ZnO NPs (68, 203, and 610 mg/kg/d) by

oral gavage. The control group was treated with the same volume of ultrapure water on PND 22 and each subsequent day for a further 28 days. Body weight and length, food intake, and water consumption were recorded. The mental state of each animal was also observed daily.

After 28 days, the blood of each rat was collected after anesthetization by ether inhalation. Blood was collected by eyeball extraction immediately after sacrifice by cervical dislocation. The rats were dissected and the liver was collected. All soft tissue was stripped from the tibia and placed in a centrifuge tube filled with 4% paraformaldehyde for fixation. Both the serum and tissue samples were stored in a freezer at −80°C until use.

Evaluation of Growth and Development

The animals were measured and weighed prior to the administration of ZnO NPs or ultrapure water. The body weight of the 32 SD rats was recorded every day. The body length of all rats was measured every 2 weeks (on days 1, 14, and 28 of exposure). Body length was measured from the tip of the nose to the tail. The length of the tibia was measured after sacrifice. The body mass index (BMI) was calculated from weight and body length (BMI = body weight/body length^2). Food intake and water consumption were also recorded.

Zn Concentration in Tissue

Liver and bone tissue (weight = 0.5–1 g) was harvested from the animals in the control and experimental groups. Each sample was placed in a mixture of HNO_3 (10 mL) and $HClO_4$ (2 mL) then heated to 230°C for 1 h. The temperature was further increased to 280°C until the liquid became clear and transparent. After cooling, 25 mL of ultrapure water was added to each sample, and then Zn concentration was measured.

Biochemical Indicator Assay

Liver function was evaluated by measurement of serum levels of aspartate aminotransferase (AST), alkaline phosphatase (ALP), and alanine aminotransferase (ALT). The serum levels of total calcium (Ca) and total phosphorus (P) were measured using a colorimetric assay in a biochemical analyzer (Roche Cobas c702). The Ca/P ratio was also measured. The methodological details have been described previously.[29]

ELISA for IGF-1

The serum level of IGF-1 was measured using an ELISA (Youersheng Biology Company, SEA050Ra). All procedures were performed by a skilled professional tester, in accordance with the manufacturer's instructions.

Micro-Computed Tomography (Micro-CT)

The tibia scanned using a micro-CT imager (SkyScan 1276, Bruker, Germany) at 85 kV, 200 μA. The projection images were reconstructed using Nrecon 1.7.3.0 software. Bone samples were analyzed following extraction of morphological data from the images using CTAn software. A number of parameters of bone morphology were used to ascertain changes in the trabecular bone using image processing software. A region of interest (ROI) was selected on the scanned micro CT images. Tissue volume (TV) refers to the total volume of ROI and bone volume (BV) refers to the volume defined as bone within the ROI. Relative bone volume (BV/TV) indicates the ratio of bone tissue volume to tissue volume, which directly reflects changes in bone mass. BMD indicates the bone mineral density within the bone tissue in the ROI. These parameters above reflect bone mass. In addition to this, micro CT is able to provide 3D imaging of the trabecular microstructure, from which trabecular number (Tb.N), trabecular thickness (Tb.Th) and trabecular separation (Tb.Sp) can be measured. These are the principal indicators for describing the spatial morphological structure of trabecular bone. Tb.N and Tb.Th decreases whereas Tb.Sp increases as osteoporosis develops. The structure model index (SMI) is defined as the degree to which the elements within a tissue are "rod-like" or "plate-like". If the trabecular bone is mostly "plate-like", the SMI is close to 0. Conversely, if the trabecular bone is mostly "rod-like", the SMI will be close to 3. Where osteoporosis has developed, trabecular bone changes from a plate-like shape to a rod-like shape, and SMI increases.

Immunohistochemistry

The tibia sections were immersed in citric acid antigen-repair buffer (pH 6.0) and placed in a microwave oven for antigen retrieval. The slides were then placed in PBS (pH 7.4) and washed three times for 5 min each on a decolorizing shaker after cooling naturally. The slides were then placed in 3% hydrogen peroxide and incubated at room temperature without light for 25 min, after which the decolorization step in the previous step was repeated. The slides were blocked using 3% BSA at room temperature for 30 min. Primary antibodies for osteoprotegerin (OPG) and receptor activator

of nuclear factor-κB ligand (RANKL) were incubated in a moist chamber at 4°C overnight. The slides were incubated with an HRP-labeled secondary antibody at room temperature for 50 min, then stained with DAB and counterstained with hematoxylin for 3 min. Images were captured using a light microscope (E100, Nikon). The percentage of positive staining within the whole field of view was quantified using Image Pro Plus (v6.0) software at 200× magnification.

Statistical Analysis

Data are expressed as means ± SD following analysis with SPSS v23.0 software using a one-way ANOVA. P values <0.05 were considered statistically significant.

Results

Analysis of Growth and Development

As shown in Figure 1A, no difference was observed in the initial weight for the four groups. For the 68 and 203 mg/kg ZnO NP samples, there was no significant difference in weight or growth rate compared with the control group over the first 6 days ($P > 0.05$). However, weight growth rate clearly decreased in the 610 and 203 mg/kg ZnO NP groups after the first 6 days ($P < 0.05$).

As shown in Figure 1B, initial body length was not significantly different between groups. After 14 days of administration of ZnO NP, body length shortened significantly compared with the control group in the 610 mg/kg ZnO NP group ($P < 0.05$). On the 28th day of exposure, the 68 and 203 mg/kg ZnO NP groups were significantly different from the 610 mg/kg ZnO NP group ($P < 0.01$), but not the control group ($P > 0.05$). The length of the tibia in the 610 mg/kg ZnO NP group was shorter than that of the control group (Figure 1C). BMI in each group was not significantly different from the control group (Figure 1D).

Zn Concentration Analysis

Zn concentration in the liver and the bone tissue increased significantly with increasing ZnO NP dosage, especially in the 610 mg/kg ZnO NP group ($P < 0.05$), which was

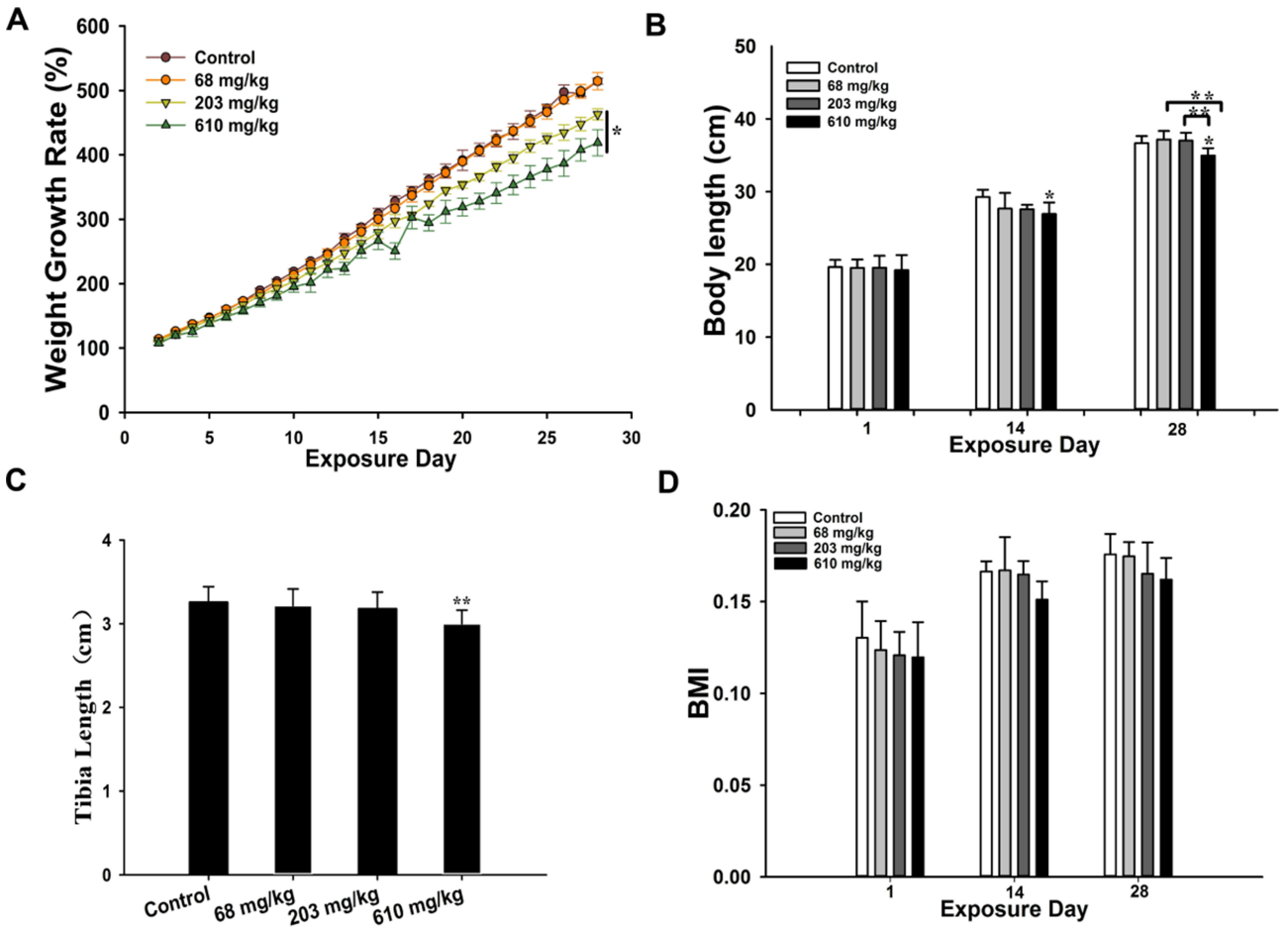

Figure 1 Characterization of growth. (**A**) Body weight growth. (**B**) Body length. (**C**) Tibia length. (**D**) Body mass index. *P<0.05, **P<0.01.

significantly higher than other experimental groups ($P < 0.05$), as shown in Figure 2A and C.

Biochemical Indicator Analysis

AST and ALT are frequently used to evaluate liver function. ALP can be used to evaluate liver and bone tissue function. As shown in Figure 2B, AST and ALT clearly increased in the 610 mg/kg ZnO NP group ($P > 0.05$), while for ALP the increase was significant ($P < 0.05$).

To examine the toxicity of ZnO NPs on bone metabolism, the concentrations of total Ca and P in serum were evaluated (Figure 2E). The Ca/P ratio was also measured, as shown in Figure 2F. The Ca/P ratio was lower in the 610 mg/kg ZnO NP group ($P < 0.05$). Serum Ca level was significantly greater in the 203 and 610 mg/kg ZnO NP groups than in the control group ($P < 0.05$) while serum P level was higher in the 610 mg/kg ZnO NP group than the control ($P<0.05$).

Analysis of IGF-1 Serum Levels

The level of IGF-1 dictates longitudinal growth of the body. Figure 2D indicates that there was no significant difference in the 68 mg/kg ZnO NP group compared with the control group. IGF-1 serum level decreased significantly in the 203 and 610 mg/kg ZnO NP groups ($P<0.05$). These results indicate that higher dosages of ZnO NPs cause lower IGF-1 serum levels.

Bone-Structure Observation by Micro-CT

Micro-CT can display the micro-architecture of bone. The 3D reconstruction of trabecular bone displayed different viewing planes for each group including coronal and transverse images. A 3D reconstruction of the tibia is shown in Figure 3A, and internal structure in the transverse direction of the proximal-tibia in Figure 3B. Non-reconstructed images are displayed in Figure 3C and D. In the control group, the bone exhibited normal external shape and structure (Figure 3A (a)). Additionally, the internal spaces of the trabecular bone in the proximal tibia metaphysis of the control group demonstrated that the cortical and trabecular bone were normal with appropriate bone mineral density (Figure 3B–D (a)). However, in the experimental groups, the shape appeared straighter, the physiological curvature changing with increasing ZnO NP dosage (Figure 3A (b–d)). The tissue within the trabecular bone declined accompanied by thinning of the cortical bone, especially in the higher ZnO NP groups (Figure 3B–D (b–d)). These results indicate that higher dosages of ZnO NPs corresponded to increasing damage to the bone tissue.

Micro-CT Data

Quantitative morphological data extracted from the micro-CT images are displayed in Figure 4 and found to be

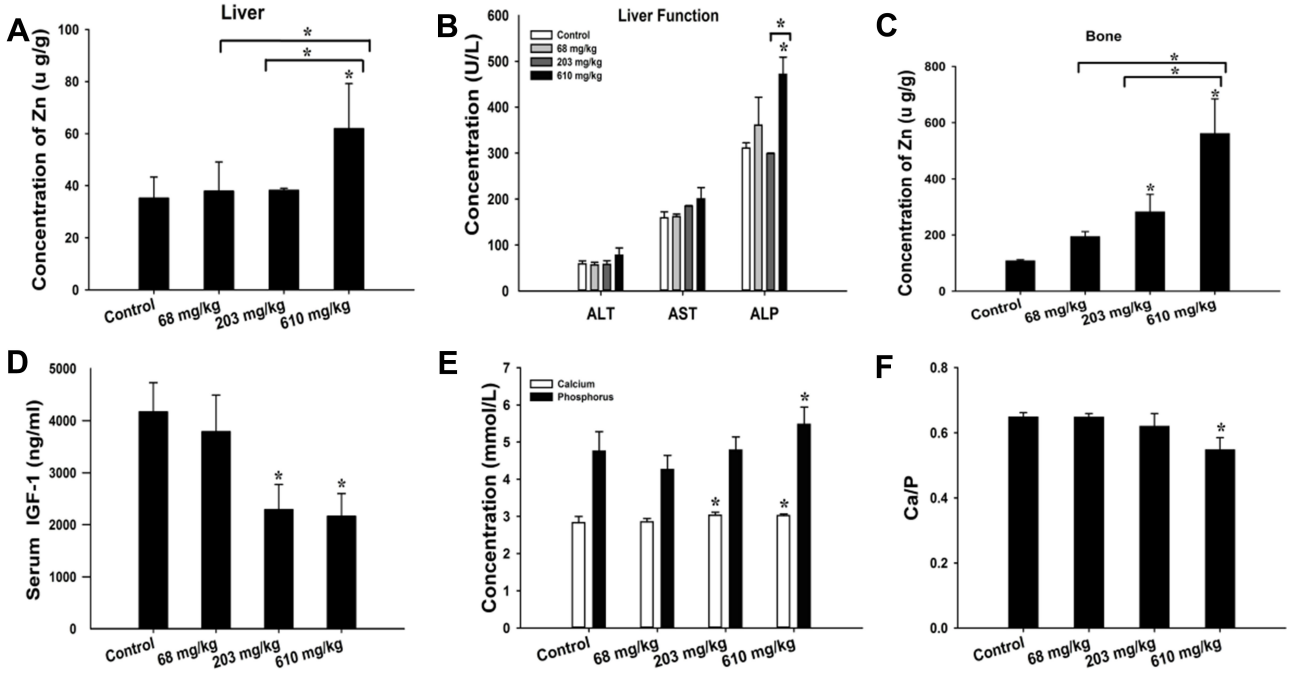

Figure 2 Analysis of biochemical indicators and accumulation of Zn. (**A**) Concentration of Zn in the liver. (**B**) Biomarkers of liver function. (**C**) Concentration of Zn in bone tissue. (**D**) Serum IGF-1 levels measured by ELISA. (**E**) Concentration of Ca and P in serum. (**F**) Ratio of Ca and P. *P<0.05 compared with control.

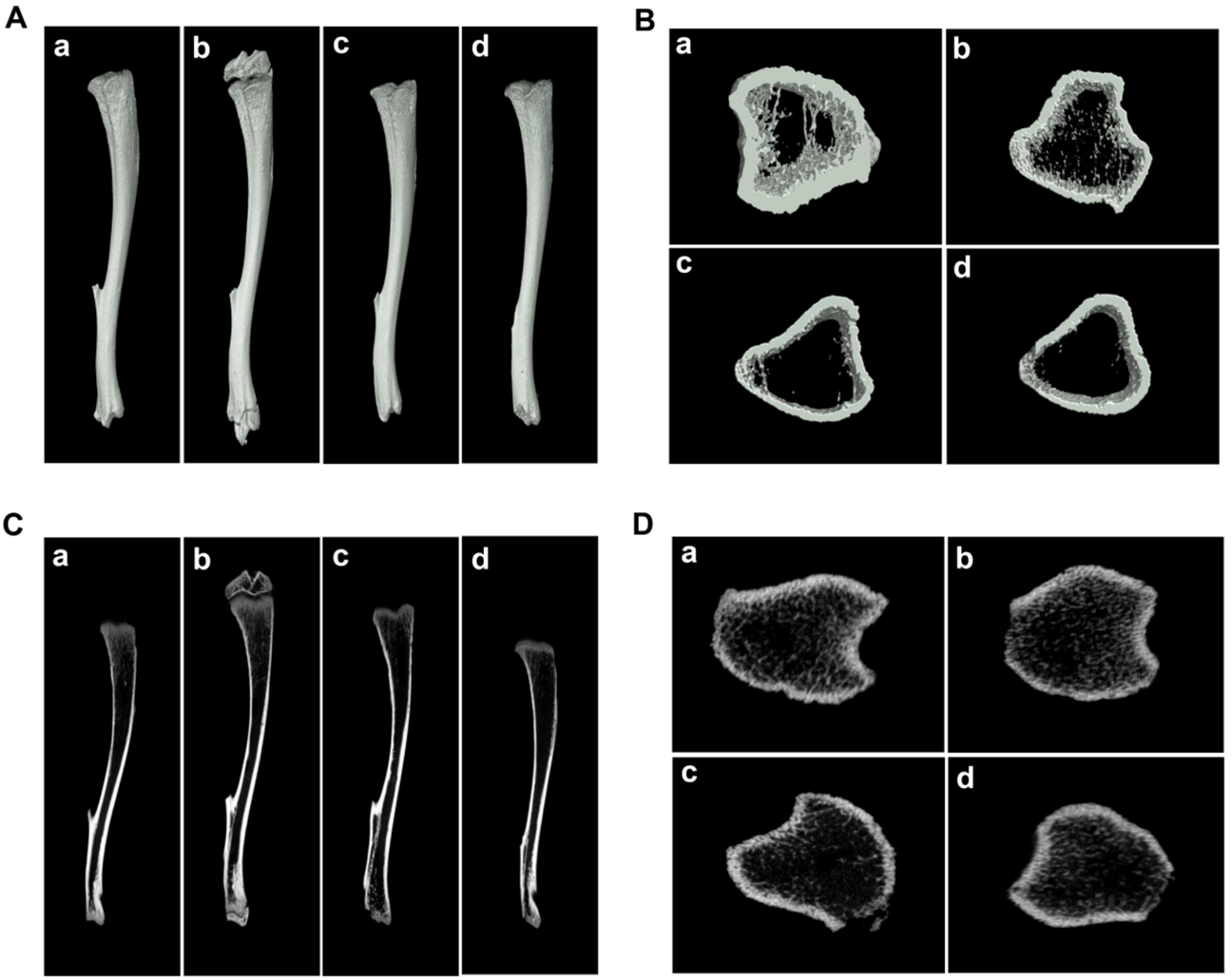

Figure 3 Micro-CT images of rat tibias. (**A**) Macroscopic 3D image reconstruction of the tibias. (**B**) 3D image reconstruction of the proximal tibias in the transverse plane. (**C**) Micro-CT images of the tibias in the coronal plane. (**D**) Micro-CT images of transverse sections of the tibias. In which: a) Control; b) 68 mg/kg ZnO NPs; c) 203 mg/kg ZnO NPs; d) 610 mg/kg ZnO NPs.

consistent with the corresponding images. With increasing ZnO NP dosage, Tb.Th decreased whereas Tb.Sp and TV increased, although not statistically different from the control group ($P>0.05$). BV was significantly lower in the 610 mg/kg ZnO NP group ($P<0.05$) compared with the control group, and BV/TV was significantly lower in the 203 and 610 mg/kg ZnO NP groups ($P<0.01$). BV/TV in the 610 mg/kg ZnO NP group was significantly lower than that of the 68 mg/kg ZnO NP group ($P<0.05$). Tb.N was significantly lower in the 68 mg/kg ZnO NP group than the control group ($P<0.05$) and very significantly lower in the 203 and 610 mg/kg ZnO NP groups ($P<0.01$). BMD was significantly lower in the 203 and 610 mg/kg ZnO NP groups ($P<0.05$). Thus, BV, BV/TV, Tb.N, and BMD were all declined as the dosage of ZnO NPs increased. SMI was significantly higher in the 203 and 610 mg/kg ZnO NP groups compared with the control group ($P<0.05$ and $P<0.01$, respectively).

OPG and RANKL Expression Levels in the Tibia

OPG and RANKL protein expression is observed as brown-yellow staining in osteoblasts (Figure 5A and B). OPG expression decreased with increasing ZnO NP dosage, the differences between the control and the 203 and 610 mg/kg ZnO NP groups being significant (Figure 5C). Additionally, RANKL expression increased with increasing ZnO NP dosage although the difference was not significant (Figure 5D). The OPG/RANKL ratio reduced in the ZnO NP treatment groups in a dose-dependent manner, and was especially apparent in the 610 mg/kg ZnO NP group (Figure 5E).

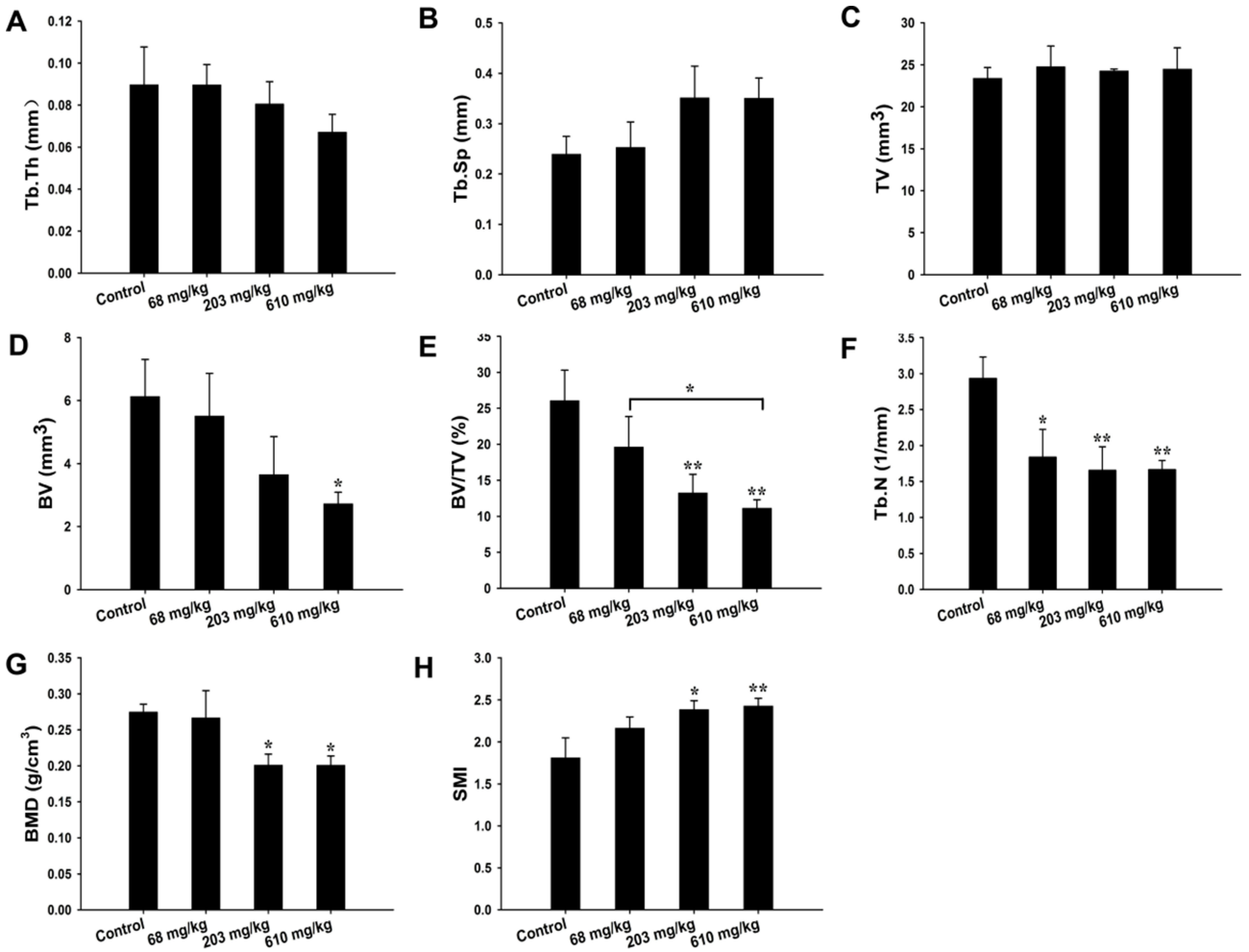

Figure 4 Quantitative morphological analysis from micro-CT images of tibias. (**A**) Trabecular thickness (Tb.Th). (**B**) Trabecular separation (Tb.Sp). (**C**) Tissue volume (TV). (**D**) Bone volume (BV). (**E**) Relative bone volume (BV/TV). (**F**) Trabecular number (Tb.N). (**G**) Bone mineral density (BMD). (**H**) Structure model index (SMI). *P<0.05, **P<0.01.

Discussion

Multiple products containing ZnO NPs are used extensively and thus may become easily ingested by children. Previous studies have explored the toxicity of ZnO NPs in the liver, ovaries, and testes of rats,[6,18] but limited research has been conducted to explore their effects on the bone tissue in young rats. In the present study, the potential risks to bone tissue of ZnO NPs by oral administration were investigated in young rats.

Body weight is a visual indicator of growth and development. As shown in Figure 1A, body weight increased less quickly in ZnO NP-exposed groups, especially in the 203 and 610 mg/kg ZnO NP groups. These results were consistent with those of Hong et al. They evaluated a range of dosages (0, 100, 200, and 400 mg/(kg·d)) of 20 nm ZnO NPs for 15 days and found that the gain in body weight was lower in the 400 mg/kg ZnO NP group.[30]

Similarly, body length, especially longitudinal growth can evaluate the growth and development of the body. A review found evidence that ZnO NPs can shorten the body length of zebrafish embryos and cause malformation.[31] In the present study, with increased duration of exposure, body length decreased in the 610 mg/kg ZnO NP group compared with the control and other ZnO NP groups (Figure 1B). Accordingly, we speculated that ZnO NPs affected longitudinal growth and that the damage caused by higher dosages of ZnO NPs occurs earlier and is more severe. The BMI results further indicate that ZnO NPs did not influence body type (Figure 1D).

A number of researchers suggest that the tibia or femur should be used as indicators of longitudinal growth.[32,33] Accordingly, we selected the tibia to assess the longitudinal growth of rats. Hong et al indicated that ZnO NPs can induce skeletal malformation, such as short ribs and incomplete ossification of the thoracic centrum in fetuses.

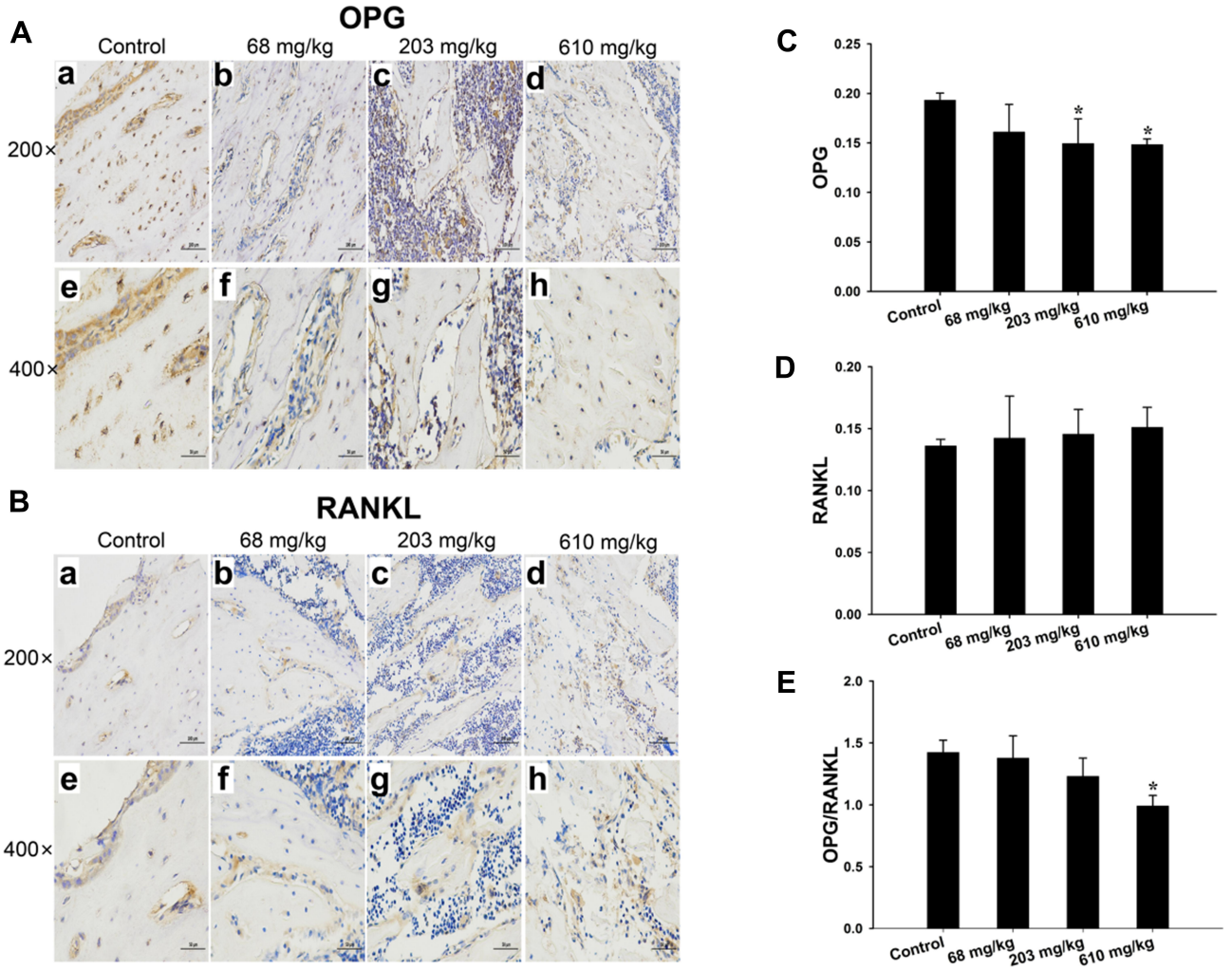

Figure 5 Immunohistochemical staining of rat tibia sections. (**A**) OPG expression stained brown-yellow in the cytoplasm of osteoblasts (200x, 400x). (**B**) RANKL-positive cells stained brown-yellow (200x, 400x). (**C**) Average optical density values of OPG expression in tibia specimens of four groups. (**D**) Average optical density values of RANKL expression in tibia specimens of four groups. (**E**) OPG/RANKL ratio. In which, a) Control, b) 68 mg/kg ZnO NPs, c) 203 mg/kgZnO NPs, d) 610 mg/kg ZnO NPs (200x); e) Control; f) 68 mg/kg ZnO NPs; g) 203 mg/kg ZnO NPs; h) 610 mg/kg ZnO NPs (400x).

However, changes in longitudinal bone were not described in Hong's study.[30] In the present investigation, tibia length was significantly different only in the 610 mg/kg ZnO NP group (Figure 1C). We concluded that tibia length was therefore only affected by high dosages of ZnO NPs.

Micro-CT was used to assess the condition of bone damage in the proximal tibia in the present study. We evaluated the biomechanical strength and risk of bone fracture. As shown in Figure 3, the proximal tibia was evaluated from two perspectives. In the experimental groups, there appeared insufficient trabeculae and thinned cortical bone combined with a changed physiological curvature when viewed in the coronal or transverse perspective. Conversely, the control group displayed a normal external shape and internal structure. Tibia micro-CT demonstrated that the trabecular bone was sparse with cortical bone becoming thinner following exposure to ZnO NP, indicating osteoporosis. We further evaluated the microstructure of the trabecular bone with a number of quantitative parameters. SMI indicates the degree of being "rod-like" or "plate-like". Conversion from plate-like to rod-like elements (SMI values tending from 0 to 3, respectively) indicates destruction of the trabecular bone structure.[34] In the present study, the value of SMI increased significantly in the 203 and 610 mg/kg ZnO NP groups, indicating the adoption of rod-like elements and that the trabecular bone structure was damaged in the high-dosage groups (Figure 4H). Combined with decreased Tb.N, Tb.Th, and BMD, we conclude that at a sufficient dosage of ZnO NPs, the biomechanical

strength of the bone decreases with an increased risk of bone fracture.

In clinical settings, patients with liver disease display decreased bone density and increased risk of bone fracture.[35] To determine why ZnO NPs inflict bone damage, we further analyzed Zn concentration in the liver and bone tissue. We found that higher dosages of ZnO NPs caused greater accumulation in the liver and bone (Figure 2A and C). Indicators of liver function, namely, AST, ALT, and ALP, increased in the 610 mg/kg ZnO NP group, indicating that liver function was affected by deposits of ZnO NPs (Figure 2B). ALP is also an indicator of bone damage. The results of 610 mg/kg ZnO NP group demonstrate significant differences compared with the control. Thus, we conclude that ZnO NPs directly affect the liver and bone tissue.

The liver is the master organ of synthesis and secretes IGF-1. We found decreased serum levels of IGF-1 in the 203 and 610 mg/kg ZnO NP groups (Figure 2D). In accordance with a previous finding that liver function is injured by ZnO NPs, we speculate that decreased IGF-1 levels were due to ZnO NP damage to liver function. Interestingly, IGF-1 is a factor critical in the regulation of longitudinal length. Bachagol et al found that longitudinal length is substantially related to serum levels of IGF-1.[14] Combined with previous results indicating that longitudinal length, including both body and tibia length, shortens with increased dosage of ZnO NPs, we speculated that the shortened longitudinal length also resulted from decreased serum level of IGF-1.

During bone formation, osteoblasts and osteoclasts are the principal cell types involved. They play important roles in bone formation and resorption.[36] Bone resorption and formation remain stable under physiological conditions such that skeletal structure and function are maintained.[37] Levels of total Ca and P in serum can also reflect changes in bone metabolism. Normally, Ca and P are relatively balanced so that normal bone structure is maintained. The normal serum level of Ca will increase due to increased osteoclast activity. As bone Ca is delivered to the blood, bone strength decreases, increasing the risk of bone fracture. In the present study, Ca levels increased in the 203 and 610 mg/kg ZnO NP groups, but there was no apparent change in P levels (Figure 2E). This finding indicates that ZnO NPs disrupt the balance between bone formation and resorption. The Ca/P ratio is an indication of the same phenomenon (Figure 2F). However, Abdelkarem et al reported that serum levels of Ca and P did not significantly differ when rats were dosed with 600 mg/kg ZnO NPs for 5 days by oral administration.[10] Herein, we found that increasing the duration of administration may increase the possibility of damage to the bone tissue. Thus, we believe that ZnO NPs disrupt the balance of bone metabolism and promote osteoclast activity.

However, the mechanism by which ZnO NPs affect osteoclasts requires further investigation. A number of studies have reported that the OPG/RANK/RANKL pathway has a close connection with the balance between osteoblasts and osteoclasts. RANKL and OPG reflect osteoclast activity. RANKL produced by osteoblasts binds to receptor activator of nuclear factor-κB (RANK) on the surface of osteoclasts resulting in increased bone resorption. Where OPG blocks RANKL to bind with RANK,[38] thereby inhibiting osteoclast activity. If RANKL were overexpressed or OPG levels were abnormally low, bone resorption would be greater than bone formation, resulting in osteoporosis. A number of studies have also shown that IGF-1 receptors exist in osteoblasts and osteoclasts, indicating that IGF-1 may directly act on osteoblasts to stimulate osteoclast function.[39] By contrast, a number of researchers have reported that the effect of IGF-1 on bone remodeling may be mediated by the OPG/RANK/RANKL system. Rubin et al found that IGF-1 decrease OPG expression but increase RANKL expression in mouse stromal cells.[40] Zhao et al drew the same conclusion.[39] However, Guerra-Menéndez et al reported that low-levels of IGF-1 can decrease OPG expression and increase RANKL expression.[41] Gorny et al demonstrated similar results and believed that differences are due to variations in cell phenotype in vitro.[42] In the present study, we drew the same conclusion that low levels of IGF-1 were accompanied by decreased OPG expression, increased RANKL expression, and therefore a low OPG/RANKL ratio, especially in the 610 mg/kg ZnO NP group, in addition to abnormal levels of Ca and Ca/P ratio. We believe that osteoclast activity increases with decreased levels of IGF-1. Overall, the results suggest that decreased OPG expression and increased RANKL expression promote osteoclast activity leading to accelerated bone loss, which may be related to reduced IGF-1 levels via the OPG/RANK/RANKL pathway. ZnO NPs affect bone growth indirectly by decreasing IGF-1 levels via abnormal liver function.

In summary, combined with abnormal liver function, higher Zn concentrations were observed in the liver and bone tissues leading to modified biochemical indicators,

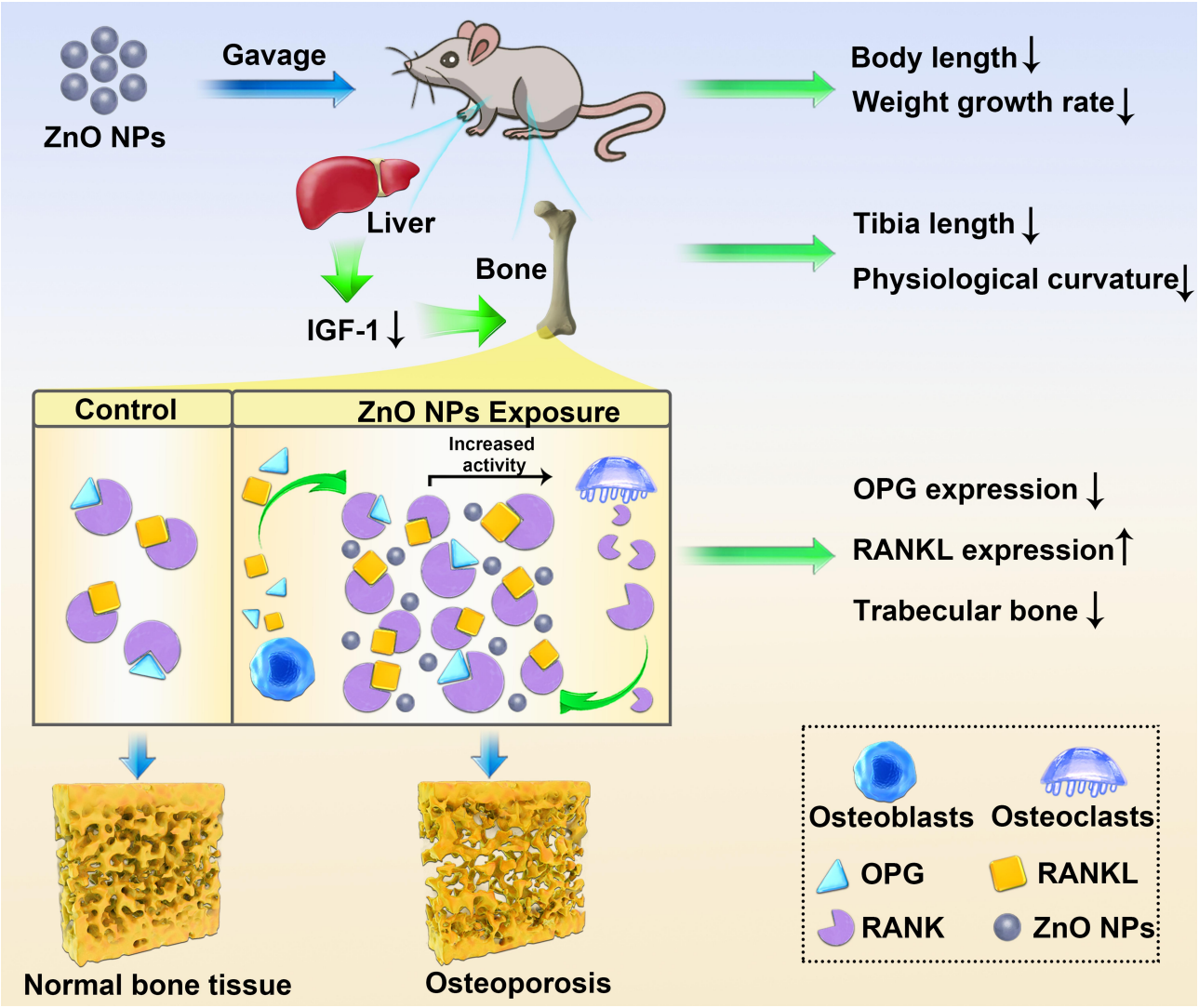

Figure 6 The schematic diagram for the ZnO NPs induced bone growth restriction in young rats through OPG/RANK/RANKL/IGF-1 pathway.

OPG, RANKL, and alteration of trabecular bone structure with a high dosage of ZnO NPs (Figures 2–5). We conclude that ZnO NPs directly or indirectly hinder bone growth through deposition in bone and by decreased levels of IGF-1. ZnO NPs may also decrease bone formation and accelerate bone loss due to the effect of the OPG/RANK/RANKL/IGF-1 pathway on bone remodeling, which led to bone growth restriction in young rats (Figure 6).

Conclusions

We evaluated the effects of different dosages of ZnO NPs on the growth of bone in young rats. The results indicate that ZnO NPs reduced the rate of weight gain and decreased the length of the body and tibias. Micro-CT analysis demonstrated that ZnO NPs exert a clear detrimental effect on the tissue within the tibia with increasing dosage, as indicated by significantly decreased BMD, Tb. N, and BV/TV. Levels of AST, ALT, and ALP, serum levels of IGF-1, the expression of OPG, and the OPG/RANKL ratio were also clearly lower in rats exposed to high-dose ZnO NPs. Changed serum Ca/P levels increased the disruption of bone-metabolism. In addition, we observed the accumulation of Zn in the liver and bone. These observations demonstrate that ZnO NPs affect bone growth in young rats by altering IGF-1 levels or by direct injury, thereby inhibiting their development. ZnO NPs can also promote osteoclast activity and bone loss, which may be due to transduction of the OPG/RANK/RANKL/IGF-1 pathway.

Acknowledgments

This work was supported by the National Natural Science Foundation of China (81771658). Xinyue Xu, Yizhou Tang, and Yuanyuan Lang are co-first authors.

Disclosure

The authors report no conflicts of interest in this work.

References

1. Vyslouzil J, Kulich P, Zeman T, et al. Subchronic continuous inhalation exposure to zinc oxide nanoparticles induces pulmonary cell response in mice. *J Trace Elem Med Biol*. 2020;61:126511. doi:10.1016/j.jtemb.2020.126511
2. Biskos G, Schmidt-Ott A. Airborne engineered nanoparticles: potential risks and monitoring challenges for assessing their impacts on children. *Paediatr Respir Rev*. 2012;13(2):79–83.
3. Das J, Choi YJ, Song H, Kim JH. Potential toxicity of engineered nanoparticles in mammalian germ cells and developing embryos: treatment strategies and anticipated applications of nanoparticles in gene delivery. *Hum Reprod Update*. 2016;22(5):588–619. doi:10.1093/humupd/dmw020
4. Lopez-Chaves C, Soto-Alvaredo J, Montes-Bayon M, Bettmer J, Llopis J, Sanchez-Gonzalez C. Gold nanoparticles: distribution, bioaccumulation and toxicity. In vitro and in vivo studies. *Nanomedicine*. 2018;14(1):1–12. doi:10.1016/j.nano.2017.08.011
5. Seaton A, Tran L, Aitken R, Donaldson K. Nanoparticles, human health hazard and regulation. *J R Soc Interface*. 2010;7(Suppl 1):S119–S129. doi:10.1098/rsif.2009.0252.focus
6. Teng C, Jia J, Wang Z, Sharma VK, Yan B. Size-dependent maternal-fetal transfer and fetal developmental toxicity of ZnO nanoparticles after oral exposures in pregnant mice. *Ecotoxicol Environ Saf*. 2019;182:109439. doi:10.1016/j.ecoenv.2019.109439
7. Peters RJB, Bouwmeester H, Gottardo S, et al. Nanomaterials for products and application in agriculture, feed and food. *Trends Food Sci Technol*. 2016;54:155–164. doi:10.1016/j.tifs.2016.06.008
8. Rajput V, Minkina T, Sushkova S, et al. ZnO and CuO nanoparticles: a threat to soil organisms, plants, and human health. *Environ Geochem Health*. 2020;42(1):147–158. doi:10.1007/s10653-019-00317-3
9. Zhao X, Wang S, Wu Y, You H, Lv L. Acute ZnO nanoparticles exposure induces developmental toxicity, oxidative stress and DNA damage in embryo-larval zebrafish. *Aquat Toxicol*. 2013;136–137:49–59.
10. Abdelkarem HM, Fadda LH, El-Sayed EM, Radwan OK. Potential role of L-arginine and vitamin E against bone loss induced by nano-zinc oxide in rats. *J Diet Suppl*. 2018;15(3):300–310. doi:10.1080/19390211.2017.1343889
11. Ma J, Zhang Z, Niu W, et al. Education, altitude, and humidity can interactively explain spatial discrepancy and predict short stature in 213,795 Chinese school children. *Front Pediatr*. 2019;7:425. doi:10.3389/fped.2019.00425
12. Quitmann JH, Bullinger M, Sommer R, Rohenkohl AC, Bernardino Da Silva NM, Li X. Associations between psychological problems and quality of life in pediatric short stature from patients' and parents' perspectives. *PLoS One*. 2016;11(4):e0153953. doi:10.1371/journal.pone.0153953
13. Mohamad MI, Khater MS. Evaluation of insulin like growth factor-1 (IGF-1) level and its impact on muscle and bone mineral density in frail elderly male. *Arch Gerontol Geriatr*. 2015;60(1):124–127. doi:10.1016/j.archger.2014.08.011
14. Bachagol D, Joseph GS, Ellur G, et al. Stimulation of liver IGF-1 expression promotes peak bone mass achievement in growing rats: a study with pomegranate seed oil. *J Nutr Biochem*. 2018;52:18–26. doi:10.1016/j.jnutbio.2017.09.023
15. Yang H, Yan K, Yuping X, et al. Bone microarchitecture and volumetric bone density impairment in young male adults with childhood-onset growth hormone deficiency. *Eur J Endocrinol*. 2019;180(2):145–153. doi:10.1530/EJE-18-0711
16. Deng Y, Cao H, Cu F, et al. Nicotine-induced retardation of chondrogenesis through down-regulation of IGF-1 signaling pathway to inhibit matrix synthesis of growth plate chondrocytes in fetal rats. *Toxicol Appl Pharmacol*. 2013;269(1):25–33. doi:10.1016/j.taap.2013.02.008
17. Hu H, Zhao X, Ma J, et al. Prenatal nicotine exposure retards osteoclastogenesis and endochondral ossification in fetal long bones in rats. *Toxicol Lett*. 2018;295:249–255. doi:10.1016/j.toxlet.2018.07.005
18. Kuang H, Yang P, Yang L, Aguilar ZP, Xu H. Size dependent effect of ZnO nanoparticles on endoplasmic reticulum stress signaling pathway in murine liver. *J Hazard Mater*. 2016;317:119–126. doi:10.1016/j.jhazmat.2016.05.063
19. Kolba N, Guo Z, Olivas FM, Mahler GJ, Tako E. Intra-amniotic administration (Gallus gallus) of TiO2, SiO2, and ZnO nanoparticles affect brush border membrane functionality and alters gut microflora populations. *Food Chem Toxicol*. 2020;135:110896. doi:10.1016/j.fct.2019.110896
20. Tang S, Wang M, Germ KE, et al. Health implications of engineered nanoparticles in infants and children. *World J Pediatr*. 2015;11(3):197–206.
21. Li J, Song Y, Vogt RD, Liu Y, Luo J, Li T. Bioavailability and cytotoxicity of cerium- (IV), copper- (II), and zinc oxide nanoparticles to human intestinal and liver cells through food. *Sci Total Environ*. 2020;702:134700. doi:10.1016/j.scitotenv.2019.134700
22. Tang Y, Chen B, Hong W, et al. ZnO nanoparticles induced male reproductive toxicity based on the effects on the endoplasmic reticulum stress signaling pathway. *Int J Nanomedicine*. 2019;14:9563–9576. doi:10.2147/IJN.S223318
23. Chen B, Hong W, Tang Y, Zhao Y, Aguilar ZP, Xu H. Protective effect of the NAC and Sal on zinc oxide nanoparticles-induced reproductive and development toxicity in pregnant mice. *Food Chem Toxicol*. 2020;143:111552. doi:10.1016/j.fct.2020.111552
24. Haase H, Overbeck S, Rink L. Zinc supplementation for the treatment or prevention of disease: current status and future perspectives. *Exp Gerontol*. 2008;43(5):394–408. doi:10.1016/j.exger.2007.12.002
25. Li CH, Shen CC, Cheng YW, et al. Organ biodistribution, clearance, and genotoxicity of orally administered zinc oxide nanoparticles in mice. *Nanotoxicology*. 2012;6(7):746–756. doi:10.3109/17435390.2011.620717
26. Chen Z, Wang Y, Zhuo L, et al. Interaction of titanium dioxide nanoparticles with glucose on young rats after oral administration. *Nanomedicine*. 2015;11(7):1633–1642. doi:10.1016/j.nano.2015.06.002
27. Quinn R. Comparing rat's to human's age: how old is my rat in people years? *Nutrition*. 2005;21(6):775–777. doi:10.1016/j.nut.2005.04.002
28. Hamner HC, Perrine CG, Scanlon KS. Usual intake of key minerals among children in the second year of life, NHANES 2003–2012. *Nutrients*. 2016;8(8):8. doi:10.3390/nu8080468
29. Li X, Liao J, Park SI, et al. Drugs which inhibit osteoclast function suppress tumor growth through calcium reduction in bone. *Bone*. 2011;48(6):1354–1361. doi:10.1016/j.bone.2011.03.687
30. Hong JS, Park MK, Kim MS, et al. Prenatal development toxicity study of zinc oxide nanoparticles in rats. *Int J Nanomedicine*. 2014;9(Suppl 2):159–171.
31. Cela P, Vesela B, Matalova E, Vecera Z, Buchtova M. Embryonic toxicity of nanoparticles. *Cells Tissues Organs*. 2014;199(1):1–23. doi:10.1159/000362163
32. Choi H, RYu K-Y, Roh J, Baea J. Effect of radioactive iodine-induced hypothyroidism on longitudinal bone growth during puberty in immature female rats. *Exp Anim*. 2018;67:395–401. doi:10.1538/expanim.18-0013

33. Foster AD. The impact of bipedal mechanical loading history on longitudinal long bone growth. *PLoS One*. 2019;14(2):e0211692.
34. Jiang Y, Zhao J, White DL, Genant HK. Micro CT and micro MR imaging of 3D architecture of animal skeleton. *J Musculoskelet Neuronal Interact*. 2000;1:45–51.
35. Nussler AK, Wildemann B, Freude T, et al. Chronic CCl4 intoxication causes liver and bone damage similar to the human pathology of hepatic osteodystrophy: a mouse model to analyse the liver-bone axis. *Arch Toxicol*. 2014;88:997–1006.
36. Mackie EJ, Ahmed YA, Tatarczuch L, Chen KS, Mirams M. Endochondral ossification: how cartilage is converted into bone in the developing skeleton. *Int J Biochem Cell Biol*. 2008;40(1):46–62. doi:10.1016/j.biocel.2007.06.009
37. Chen X, Wang Z, Duan N, Zhu G, Schwarz EM, Xie C. Osteoblast-osteoclast interactions. *Connect Tissue Res*. 2018;59(2):99–107. doi:10.1080/03008207.2017.1290085
38. Hofbauer LC. Pathophysiology of RANK ligand (RANKL) and osteoprotegerin (OPG). *Ann Endocrinol*. 2006;67(2):139–141. doi:10.1016/S0003-4266(06)72569-0
39. Zhao HY, Liu JM, Ning G, et al. Relationships between insulin-like growth factor-I (IGF-I) and OPG, RANKL, bone mineral density in healthy Chinese women. *Osteoporos Int*. 2008;19(2):221–226. doi:10.1007/s00198-007-0440-y
40. Rubin J, Ackert-Bicknell CL, Zhu L, et al. IGF-I regulates osteoprotegerin (OPG) and receptor activator of nuclear factor-kappaB ligand in vitro and OPG in vivo. *J Clin Endocrinol Metab*. 2002;87(9):4273–4279. doi:10.1210/jc.2002-020656
41. Guerra-Menéndez L, Sádaba MC, Puche JE, et al. IGF-I increases markers of osteoblastic activity and reduces bone resorption via osteoprotegerin and RANK-ligand. *J Transl Med*. 2013;11:271. doi:10.1186/1479-5876-11-271
42. Gorny G, Shaw A, Oursler MJ. IL-6, LIF, and TNF-alpha regulation of GM-CSF inhibition of osteoclastogenesis in vitro. *Exp Cell Res*. 2004;294(1):149–158. doi:10.1016/j.yexcr.2003.11.009